Available online at www.sciencedirect.com

SciVerse ScienceDirect

Ceramics International 39 (2013) S189–S193

CERAMICS INTERNATIONAL

www.elsevier.com/locate/ceramint

Electrical properties of chemical solution deposited $(Bi_{0.9}RE_{0.1})(Fe_{0.975}Cu_{0.025})O_{3-\delta}$ (RE=Ho and Tb) thin films

Jin Won Kim[a], Chinanmbedu Murugesan Raghavan[a], Youn-Jang Kim[a], Jeong-Jung Oak[a], Hae Jin Kim[a], Won-Jeong Kim[a], Myong Ho Kim[b], Tae Kwon Song[b], Sang Su Kim[a,*]

[a] *Department of Physics Changwon National University, Changwon, Gyeongnam 641-773, Republic of Korea*
[b] *School of Nano & Advanced Materials Engineering, Changwon National University, Changwon, Gyeongnam 641-773, Republic of Korea*

Abstract

Pure $BiFeO_3$ (BFO) and $(Bi_{0.9}RE_{0.1})(Fe_{0.975}Cu_{0.025})O_{3-\delta}$ (RE=Ho and Tb, denoted by BHFCu and BTFCu) thin films were prepared on Pt(111)/Ti/SiO_2/Si(100) substrates by using a chemical solution deposition method. The BHFCu and BTFCu thin films showed improved electrical and ferroelectric properties compared to pure BFO thin film. Among them, the BTFCu thin film exhibited large remnant polarization ($2P_r$), low coercive field ($2E_c$) and reduced leakage current density, which are 89.15 C/cm^2 and 345 kV/cm at 1000 kV/cm and 5.38×10^{-5} A/cm^2 at 100 kV/cm, respectively.

Keywords: A. Films; C. Electrical properties; C. Ferroelectric properties

1. Introduction

Multiferroic $BiFeO_3$ (BFO) plays an important role in the fabrication of electronic devices, such as ferroelectric random access memories, spintronics and sensors. BFO is the only material that exhibits magnetoelectric effect at room temperature due to its high Curie ($T_c \sim 810$ °C) and Néel ($T_N \sim 380$ °C) transition temperatures [1,2]. Even though BFO shows superior ferroelectric properties, the low electrical resistivity due to large leakage current has much influence on the device performance. The origin of the leakage current is believed to originate from volatilization of Bi ion, small amount of Fe^{2+} ion and oxygen vacancies [3,4]. Defect engineering (partial substitution of rare earth and/or transition metal ions) has been strongly recommended to reduce the leakage current and increase the ferroelectric properties and there have been many reports to reduce the leakage current in the BFO thin film [3–6]. Among the reports, there are a few papers on holmium (Ho) and terbium (Tb) doped BFO in bulk system, detailed reports on the ferroelectric properties of Ho and Tb with transition metal ion co-doped BFO thin films are limited [7].

In this study, the pure $BiFeO_3$ and the $(Bi_{0.9}RE_{0.1})(Fe_{0.975}Cu_{0.025})O_{3-\delta}$ (RE=Ho and Tb) thin films were prepared on Pt(111)/Ti/SiO_2/Si(100) substrates by using a chemical solution deposition method. The effects of Ho, Cu and Tb, Cu co-doping on the micro-structure, the electrical properties and the ferroelectric properties of the BFO thin film are investigated.

2. Experimental procedures

The pure $BiFeO_3$ (BFO) and the $(Bi_{0.9}RE_{0.1})(Fe_{0.975}Cu_{0.025})O_{3-\delta}$ (RE=Ho and Tb, denoted by BHFCu and BTFCu) thin films were prepared on Pt(111)/Ti/SiO_2/Si(100) substrates by using a chemical solution deposition method. The raw materials used for the precursor solutions are bismuth nitrate pentahydrate, iron nitrate nonahydrate, holmium nitrate hexahydrate, terbium nitrate hexahydrate and copper nitrate hydrate. 2-methoxyethanol and ethylene glycol were used as solvents and acetic acid was used as a catalyst. Initially, bismuth nitrate pentahydrate (5 mol% excess) was dissolved in 2-methoxyethanol and ethylene glycol mixed solvent at 40 °C

---

*Corresponding author. Tel.: +82 552133421; fax: +82 552670264.
E-mail address: skim@changwon.ac.kr (S.S. Kim).

0272-8842/$ - see front matter © 2012 Elsevier Ltd and Techna Group S.r.l. All rights reserved.
http://dx.doi.org/10.1016/j.ceramint.2012.10.060

for 30 min to make a homogeneous solution. Acetic acid was added to the bismuth solution and dissolved completely by stirring for 30 min at 40 °C. Finally, iron nitrate nonahydrate was added to form the BFO solution. For the doping experiment, before the addition of iron nitrate nonahydrare, holmium nitrate hexahydrate or terbium nitrate hexahydrate was added to the bismuth solution and stirred for 30 min. Then, iron nitrate nonahydrate was dissolved to the bismuth–holmium and bismuth–terbium solutions and stirred at 40 °C for 30 min. Finally, copper nitrate hydrate was dissolved into the bismuth–holmium–iron and bismuth–terbium–iron solutions by constant stirring and the resulting BFO, BHFCu and BTFCu solutions were continuously stirred for 3 h.

The pure BFO, BHFCu and BTFCu thin films were deposited on Pt(111)/Ti/SiO_2/Si(100) substrates with the precursor solutions by using a spin-coating method at a spinning rate of 3500 rpm for 25 s. The wet films were prebaked on a hot-plate at 360 °C for 10 min. The coating and the baking processes were repeated for 12 times to obtain a desired film thickness. And then, the coated films were annealed at 550 °C for 30 min under a nitrogen atmosphere for crystallization.

The polycrystalline structures of the BFO, BHFCu and BTFCu thin films were confirmed by using an X-ray diffractometer (Rigaku, MiniFlex II LMH) and a Raman spectroscope (Jasco, NRS-3100). The surface morphologies and the cross-sectional micrographs of the pure BFO, BHFCu and BTFCu thin films were obtained by using a field emission scanning electron microscope (MIRA II LMH, H.S). In order to study the electrical properties, platinum (Pt) electrodes with areas of $2.2 \times 10^{-4}\ cm^2$ were deposited on the top surfaces of the thin films by using a metal shadow mask to form a capacitor structure. Ferroelectric hysteresis loops were measured by using a standardized ferroelectric test system (Modified Sawyer–Tower circuit with an oscilloscope). The electrometer (Keithley, 6517A) was used to measure the leakage currents of the pure BFO, BHFCu and BTFCu thin films.

3. Results and discussion

The X-ray diffraction patterns of the pure BFO and the $(Bi_{0.9}RE_{0.1})(Fe_{0.975}Cu_{0.025})O_{3-\delta}$ (RE=Ho and Tb, denoted by BHFCu and BTFCu) thin films are shown in Fig. 1(a). The reflection peaks of the thin films were indexed with reference to the single-phase polycrystalline rhombohedral perovskite structure. No impurity phases were detectable in our thin films. However, the deep investigation shows the mild higher angle shift in the peak positions at $2\theta=22.5°$ and 32.0° for the BHFCu and BTFCu thin films (Fig. 1(b and c)). The split peaks of (110)/$(1\bar{1}0)$ in the pure BFO thin film were merged and appeared as broad peak around 32° for the co-doped thin films, which indicates slight changes in lattice parameters due to relatively small ionic radius of Ho^{3+} ion (for 12 coordination radius 0.123 nm) and Tb^{3+} ion (for 12 coordination radius 0.127 nm) than that of Bi^{3+} ion (for 12 coordination radius 0.145 nm) [8].

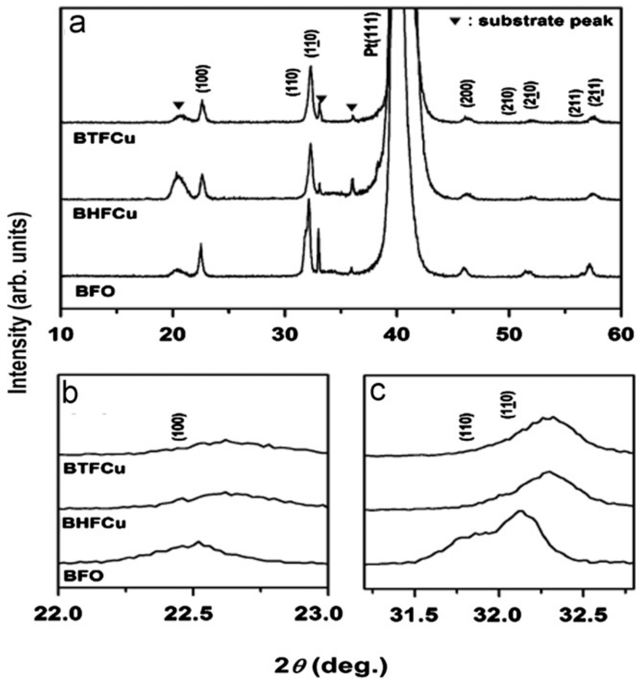

Fig. 1. (a) X-ray diffraction (XRD) patterns of the BFO, BHFCu and BTFCu thin films and (b) and (c) show the magnified XRD patterns in the vicinities of $2\theta=22.5°$ and 32°, respectively.

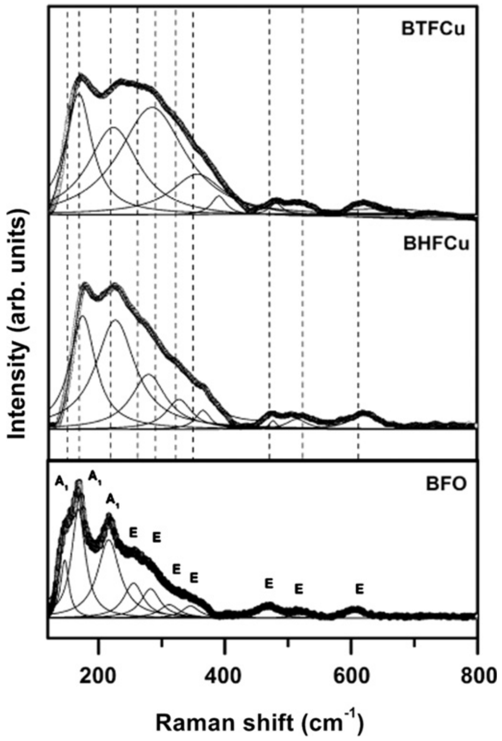

Fig. 2. Raman scattering spectra of the BFO, BHFCu and BTFCu thin films measured at room temperature. Curve fitting and deconvolution into individual peaks are shown by the thinner lines.

Fig. 2 show the Raman scattering spectra of the pure BFO, BHFCu and BTFCu thin films measured at room temperature. According to the group theory, there are 13 Raman active modes ($4A_1+9E$) are predicted for the rhombohedrally distorted *R3c* space group [9]. In the pure BFO, low frequency A_1 and high frequency E modes corresponds to the Bi–O and the Fe–O vibrations, respectively. For the co-doped thin films, the peak broadening and the intensity changes were observed in the low frequency region, which indicate substitution of rare earth metal ion into Bi site of the BFO [10]. The bond dissociation energies of the Ho–O bond (606 kJ/mol) and the Tb–O bond (694 kJ/mol) are stronger than that of the Bi–O bond (337 kJ/mol) [11]. The substitution of Ho and Tb into Bi site can stabilize the perovskite structure and compensate oxygen vacancies by controlling the evaporation of Bi ion. Both the XRD and the Raman analysis results clearly revealed the structural distortion in the co-doped thin films.

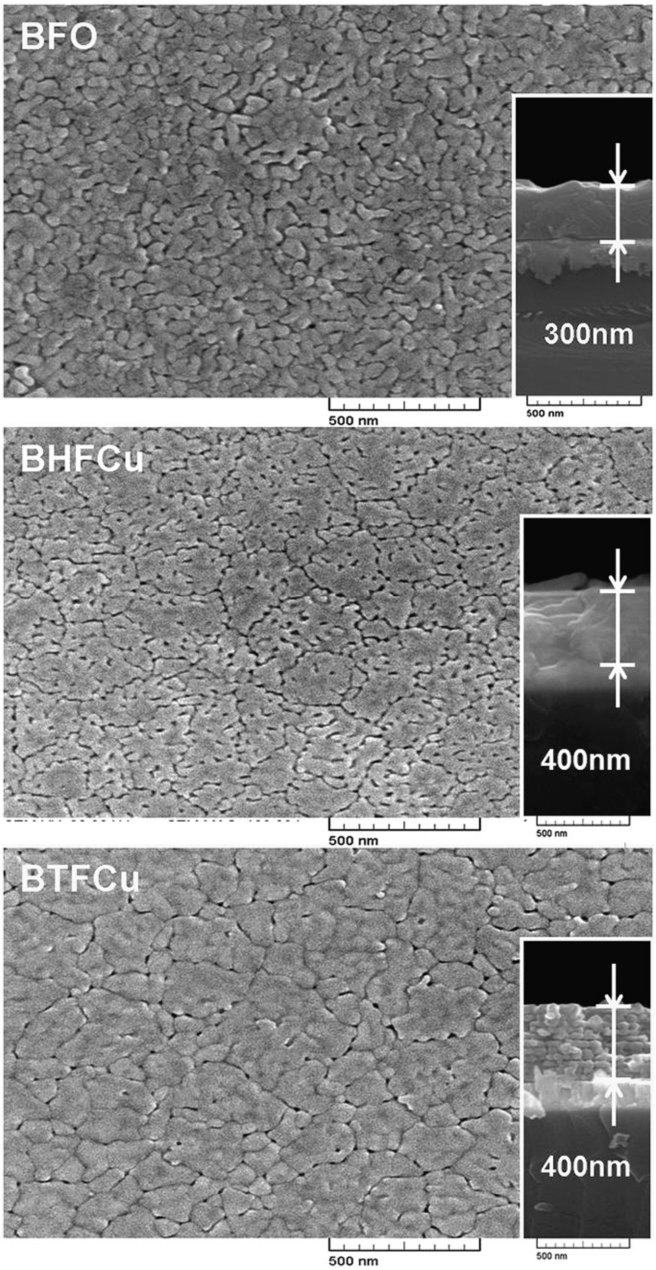

Fig. 3. Surface morphologies and cross-sectional micrographs of the BFO, BHFCu and BTFCu thin films.

The surface morphologies and the cross-sectional micrographs of the pure BFO, BHFCu and BTFCu thin films are shown in Fig. 3. In the surface morphologies, the grain size of the BHFCu and BTFCu thin films increased and formed dense micro-structure compared to the pure BFO. The grain size and the surface roughness affect electrical properties of the thin films. Hence, electrical properties of the BHFCu and BTFCu thin film are expected to be better than that of the pure BFO thin film. The thicknesses of the pure BFO, BHFCu and BTFCu thin films were 300 nm, 400 nm and 400 nm, respectively.

Fig. 4(a) shows the leakage current densities with applied electric field for the pure BFO and the co-doped thin films measured at room temperature. The measured leakage current densities of the pure BFO, BHFCu and BTFCu thin films were 2.58×10^{-3}, 2.06×10^{-4} and 5.38×10^{-5} A/cm^2 at an applied electric field of 100 kV/cm, respectively. The BFO thin film exhibits high leakage current density, because of poor microstructure, volatilization of Bi ion, Fe^{2+} ion, oxygen vacancies and nonstoichiometry. Formations of oxygen vacancy and Fe^{2+} ion are expressed using the Kröger–Vink notations as follows

$$2Bi_{Bi}^{\times}+2Fe_{Fe}^{\times}+6O_{O}^{\times}\rightarrow 2Bi_{Bi}^{\times}+2\mathit{Fe}'_{Fe}+5O_{O}^{\times}+V_{O}^{\bullet\bullet} \tag{1}$$

$$2Bi_{Bi}^{\times}+3O_{O}^{\times}\rightarrow 2V_{Bi}'''+3V_{O}^{\bullet\bullet}+Bi_2O_3 \tag{2}$$

where $Bi_{Bi}^{\times}$, $Fe_{Fe}^{\times}$ and $O_{O}^{\times}$ are the Bi, Fe and oxygen ions in the lattice, V_{Bi}''' and $V_{O}^{\bullet\bullet}$ indicate Bi and oxygen vacancies with three negative and two positive charges, respectively, Fe'_{Fe}

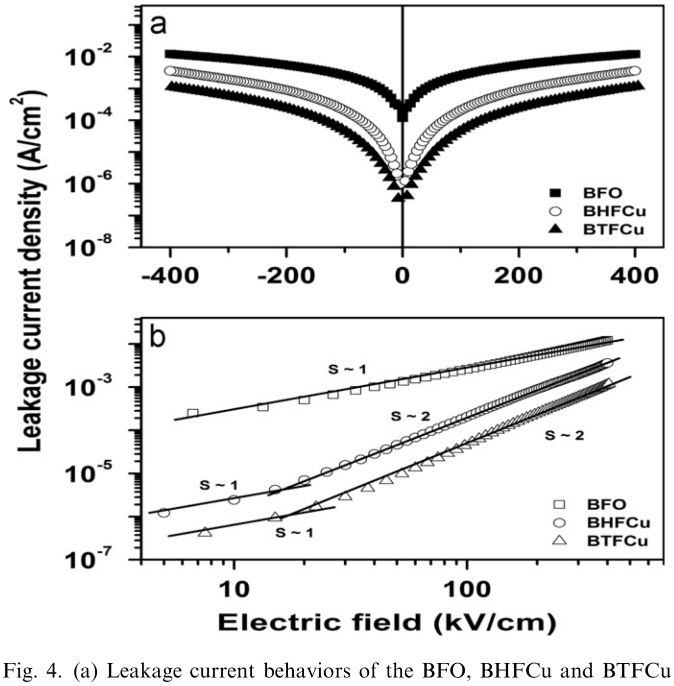

Fig. 4. (a) Leakage current behaviors of the BFO, BHFCu and BTFCu films. (b) Leakage current density versus electric field in a logarithmic scale of the BFO, BHFCu and BTFCu thin films.

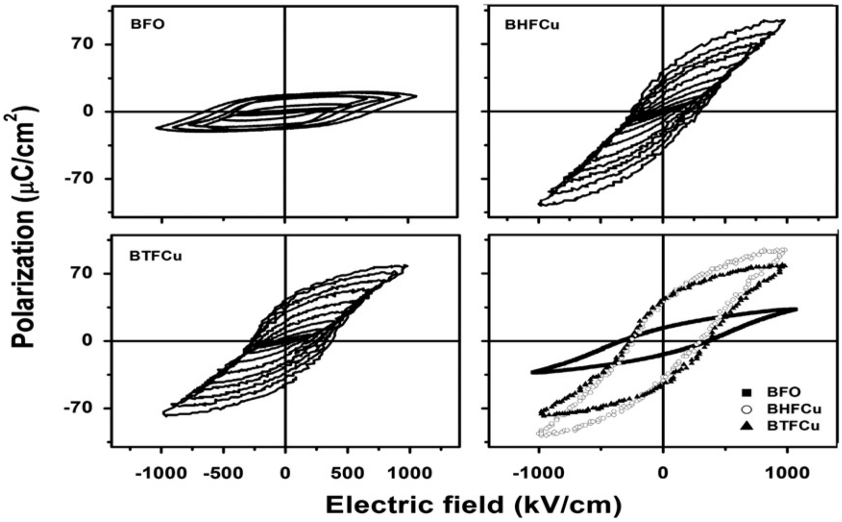

Fig. 5. Ferroelectric *P–E* hysteresis loops of the BFO, BHFCu and BTFCu thin films measured at 10 kHz.

represents an Fe^{2+} ion with one negative charge. The reduced leakage current density in the BHFCu and BTFCu thin films are consistent with reduced defects, such as oxygen vacancy and Fe^{2+} ion, and improved microstructure by the co-doping elements [6].

In order to understand the origin of leakage current, the leakage current mechanisms for the pure BFO and co-doped thin films were investigated. The $\log(J)-\log(E)$ plots are shown in Fig. 4(b). At low electric field, the slopes for the pure BFO, BHFCu and BTFCu thin films were observed to be linearly proportional to the applied electric field. The linearity of the line (slope $S \sim 1$) over the entire region in all samples implies Ohmic conduction mechanism. However, at high electric field, the leakage current density versus applied electric field exhibits non-linear behavior, which suggests that there could be different mechanism from Ohmic conduction observed at low electric fields. The change of conduction mechanism from Ohmic to space charge limited conduction has been observed above 15 kV/cm for the BHFCu and BTFCu thin films [12].

Fig. 5 shows the ferroelectric polarization–electric field (*P–E*) hysteresis loops of the pure BFO, BHFCu and BTFCu thin films measured at 10 kHz with triangular pulses. The values of remnant polarization ($2P_r$) and coercive electric field ($2E_c$) of the BFO thin film were 35 μC/cm² and 1363 kV/cm at an applied electric field of 1066 kV/cm, respectively. The improved ferroelectric properties have been observed in the BHFCu and BTFCu thin film. The values of $2P_r$ and $2E_c$ for the BHFCu and BTFCu thin films were 84 μC/cm², 542 kV/cm and 89 μC/cm², 645 kV/cm at an applied electric field of 1000 kV/cm, respectively.

4. Conclusions

In summary, the $BiFeO_3$ (BFO) and the $(Bi_{0.9}RE_{0.1})(Fe_{0.975}Cu_{0.025})O_{3-\delta}$ (RE=Ho and Tb, BHFCu and BTFCu) thin films were prepared on $Pt(111)/Ti/SiO_2/Si$ substrates by using a chemical solution deposition method. The greater structural distortion in the rhombohedral perovskite crystal structure for the BHFCu and BTFCu thin films was confirmed by using an XRD and a Raman scattering analysis. The improved ferroelectric properties and the reduced leakage current density observed in the BHFCu and BTFCu thin films are well correlated with the improved micro-structure and the reduced number of defects, such as oxygen vacancy. Hence, the co-doped BHFCu and BTFCu thin films are recommended for the fabrication of nonvolatile memory devices.

Acknowledgments

This work was supported by Priority Research Centers Program through the National Research Foundation of Korea (NRF) (2010-0029634) funded by the Ministry of Education, Science and Technology.

References

[1] L.W. Martin, Y.-H. Chu, R. Ramesh, Advances in the growth and characterization of magnetic, ferroelectric, and multiferroic oxide thin films, Materials Science and Engineering: R 68 (2010) 89–133.

[2] Y. Xu, M. Shen, Structure and optical properties of nanocrystalline $BiFeO_3$ films prepared by chemical solution deposition, Materials Letters 62 (2008) 3600–3602.

[3] G.L. Yuan, S.W. Ora, Enhanced piezoelectric and pyroelectric effects in single-phase multiferroic $Bi_{1-x}Nd_xFeO_3$ (x=0–0.15) ceramic, Applied Physics Letters 88 (2006) 062905.

[4] Q. Ke, X. Lou, Y. Wang, J. Wang, Oxygen-vacancy-related relaxation and scaling behaviors of $Bi_{0.9}La_{0.1}Fe_{0.98}Mg_{0.02}O_3$ ferroelectric thin films, Physical Review B 82 (2010) 024102.

[5] Z.X. Cheng, X.L. Wang, S.X. Dou, Improved ferroelectric properties in multiferroic $BiFeO_3$ thin films through La and Nb codoping, Physical Review B 77 (2008) 092101.

[6] H. Naganuma, J. Miura, S. Okamura, Ferroelcetric, electrical and magnetic properties of Cr, Mn, Co, Ni, Cu added polycrystalline $BiFeO_3$ films, Applied Physics Letters 93 (2008) 052901.

[7] N. Jeon, D. Rout, I.W. Kim, S.-J.L. Kang, Enhanced multiferroic properties of single-phase $BiFeO_3$ bulk ceramics by Ho doping, Applied Physics Letters 98 (2011) 072901.

[8] R.D. Shanon, Revised effective ionic radii and systematic studies of interatomic distances in halides and chalcogenide, Acta Crystallographica A32 (1976) 751–767.

[9] M.K. Singh, H.M. Jang, S. Ryu, M.–H. Jo, Polarized Raman scattering of multiferroic $BiFeO_3$ epitaxial films with rhombohedral $R3c$ symmetry, Applied Physics Letters 88 (2006) 042907.

[10] G. Kartopu, A. Lahmar, S. Habouti, C.-L. Solterbeck, B. Elouadi, M. Es-Souni, Observation of structural transitions and Jahn–Teller distortion in $LaMnO_3$-doped $BiFeO_3$ thin films, Applied Physics Letters 92 (2008) 151910.

[11] J.A. Dean, Lange's Handbook of Chemistry, 15th ed., McGraw-Hill, New York, 1999.

[12] Z. Zhonga, H. Ishiwara, Variation of leakage current mechanisms by ion substitution in $BiFeO_3$ thin films, Applied Physics Letters 95 (2009) 112902.